Indirect Lung Absorbed Dose Verification by ^{90}Y PET/CT and Complete Lung Protection by Hepatic Vein Balloon Occlusion: Proof of Concept

Yung Hsiang Kao[1], Calvin Gan[2], Alicia Corlett[1], Alexander Rhodes[2], Dinesh Sivaratnam[1], and Beng Ghee Lim[2]

[1]*Department of Nuclear Medicine, Royal Melbourne Hospital, Parkville, Victoria, Australia; and* [2]*Department of Radiology, Royal Melbourne Hospital, Parkville, Victoria, Australia*

Postradioembolization lung absorbed dose verification was historically problematic and impractical in clinical practice. We devised an indirect method using ^{90}Y PET/CT. **Methods:** Conceptually, true lung activity is simply the difference between the total prepared activity minus all activity below the diaphragm and residual activity within delivery apparatus. Patient-specific lung mass is measured by CT densitovolumetry. True lung mean absorbed dose is calculated by MIRD macrodosimetry. **Results:** Proof of concept is shown in a hepatocellular carcinoma patient with a high lung shunt fraction of 26%, where evidence of technically successful hepatic vein balloon occlusion for radioembolization lung protection was required. Indirect lung activity quantification showed the postradioembolization lung shunt fraction to be reduced to approximately 1% with a true lung mean absorbed dose of approximately 1 Gy, suggesting complete lung protection by hepatic vein balloon occlusion. **Conclusion:** We discuss possible clinical applications such as lung absorbed dose verification, refining the limits of lung tolerance, and the concept of massive activity radioembolization.

Key Words: radioembolization; selective internal radiation therapy; lung shunt fraction; ^{90}Y PET/CT; hepatic vein balloon occlusion

J Nucl Med Technol 2022; 50:240–243
DOI: 10.2967/jnmt.121.263422

Despite decades of radioembolization, the true tolerance limit of the lung to radioembolization has not yet been properly defined and to date has only been estimated by ^{99m}Tc-macroaggregated albumin (^{99m}Tc-MAA) or extrapolated from the experiences of external-beam radiotherapy (*1*). This problem is compounded by different methods of imaging and calculating the lung shunt fraction, lung mass, and radiobiologically distinct microsphere devices (*1*).

In the past decade, ^{90}Y PET with contemporaneous CT (^{90}Y PET/CT) has rapidly evolved to become the current standard of care in postradioembolization verification of tumor and nontumorous liver absorbed doses and in detection of nontarget abdominal activity (*2,3*). However, direct lung ^{90}Y PET/CT is much more problematic. First, lung radioconcentration within a PET field of view is usually low because the prescribed lung mean absorbed dose is limited to less than 20–25 Gy, resulting in noisy, quantitatively inaccurate lung scans (*1,2,4*). Second, increasing lung scan time to improve count statistics is impractical. Abdominal ^{90}Y PET/CT of 1–2 bed positions requires 20–40 min. Doubling lung scan time over 2 bed positions could take 40–80 min just for lungs alone, intolerable for any patient. Third, dedicating 60–120 min of scanner time for a single patient costs the throughput equivalent of approximately 3–6 oncology PET patients, which is difficult to justify financially.

MATERIALS AND METHODS

Dosimetric Concept

Conceptually, the true lung activity is simply the difference between the total prepared activity minus all activity below the diaphragm and residual activity within the delivery apparatus (*5*). Here, true lung activity is expressed as an equation, where radiomicrospheres are permanent implants within a closed system where all injected activity is conserved and activity leeching is negligible:

$$A_{Total} = A_{Lung} + A_{PTV} + A_{Nontarget} + A_{Residual}$$
$$\text{i.e.,}\ A_{Lung} = A_{Total} - (A_{PTV} + A_{Nontarget} + A_{Residual}),$$

where A_{Total} is total prepared activity, A_{Lung} is lung activity, A_{PTV} is activity within all planning target volumes, $A_{Nontarget}$ is abdominal nontarget activity (if any), and $A_{Residual}$ is residual activity within the delivery apparatus. The term *planning target volume* refers to all targeted arterial territories encompassing tumor and nontumorous liver (*6*). All measured activities are decay-corrected to the time of radioembolization. The lung mean absorbed dose is calculated by MIRD macrodosimetry assuming uniform activity biodistribution, using the ^{90}Y absorbed dose coefficient 50 Gy per GBq/kg (*2,6*):

$$D_{Lung} = 50 \times (A_{Lung}/M_{Lung})$$

where D_{Lung} is true lung mean absorbed dose (Gy), A_{Lung} is lung activity (GBq), and M_{Lung} is patient-specific lung mass (kg) measured by CT densitovolumetry (*7*).

Clinical Proof of Concept

We demonstrated clinical proof of concept in a hepatocellular carcinoma patient with high lung shunt fraction, where we implemented lung protection during radioembolization by hepatic vein balloon occlusion but required objective proof of technical success. This success was eventually proven by the indirect method described

Received Oct 21, 2021; revision accepted Mar. 7, 2022.
For correspondence or reprints, contact Yung Hsiang Kao (yung.kao@mh.org.au).
Published online Apr. 19, 2022.

here. We considered lung protection to be complete if the extent of hepatopulmonary shunting was reduced to a clinically negligible level (i.e., ~1%). This report has been approved by the institutional review board. The patient consented to the radioembolization planning, treatment, and this publication.

An 82-y-old man with a large, inoperable 12-cm hepatocellular carcinoma occupying segments 4 and 8 (Fig. 1A) was referred for ^{90}Y resin microsphere radioembolization (SIR-Spheres; Sirtex Medical Limited). Exploratory hepatic angiography with radiomicrosphere simulation confirmed hypervascularity with good tumoral ^{99m}Tc-MAA implantation. However, planar liver–lung scintigraphy showed a high lung shunt of 26% (Fig. 1B). We proceeded with radioembolization by implementing 2 methods of lung protection. First, activity prescription was limited to a lung safety tolerance of 20 Gy, planned by the MIRD method (i.e., partition model) (*4,6*). Second, hepatic vein occlusion of the right and middle hepatic veins was performed before radiomicrosphere infusion to minimize hepatopulmonary shunting; this method has the additional benefit of improving the tumor mean absorbed dose by retaining radiomicrospheres within tumor instead of radiomicrospheres being shunted to the lung (*8*).

For hepatic vein balloon occlusion, LeMaitre 6F Over-the-Wire Embolectomy Catheters (LeMaitre Vascular) were placed in the right and middle hepatic veins (catheter length, 80 cm; guidewire, 0.088 cm) under fluoroscopic guidance via the right internal jugular vein (*8*). Balloons were inflated before radiomicrosphere infusion, with complete occlusion of the right and middle hepatic veins visually confirmed with contrast injection (Fig. 1C). Total balloon inflation time was approximately 20 min during radioembolization (Fig. 1D). Despite visual confirmation of balloon occlusion, there remains the possibility of an unknown and invisible amount of in-transit venous radiomicrospheres temporarily suspended proximal to the inflated balloons, potential for radiomicrosphere dislodgment from tumor into the lungs after balloon deflation, and unknown lung shunt contribution by the patent left hepatic vein. All of these uncertainties require postradioembolization confirmation of the true lung activity to ensure patient safety.

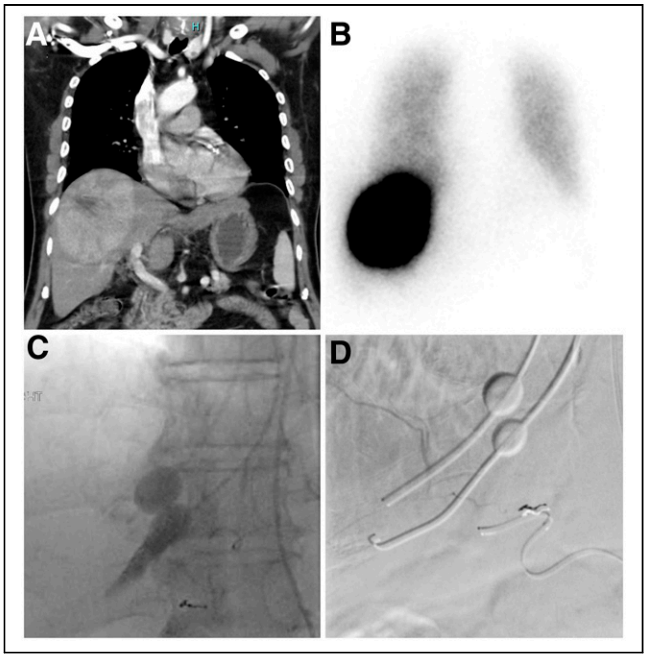

FIGURE 1. (A) CT coronal view shows a large inoperable hepatocellular carcinoma. (B) Planar liver–lung imaging showed a high lung shunt fraction of 26% estimated by ^{99m}Tc-MAA. (C) Fluoroscopy of right and middle hepatic vein balloon occlusion depicts contrast injection within the middle hepatic vein to visually confirm complete occlusion. (D) Fluoroscopy of hepatic vein occlusion balloons in their final inflated positions prior to radiomicrosphere infusion.

Postradioembolization bremsstrahlung planar imaging did not show any visually significant lung activity, a qualitative indication of successful lung protection (Fig. 2A). ^{90}Y PET/CT of the abdomen and delivery apparatus (including catheters, occlusion balloons, and drapes) was performed separately, using the Biograph Horizon (Siemens), as a gradual sweep over 20 min to image the whole liver and delivery apparatus (*2,5*). ^{90}Y PET images were reconstructed using the TrueX time-of-flight iterative algorithm (Siemens), 3 iterations and 10 subsets, a gaussian filter of 5 mm in full width at half maximum, and a 180 × 180 matrix. Low-dose CT was performed for localization, attenuation correction, and scatter correction. Images were displayed in 3-mm slice thickness and analyzed using SyngoVia software (Siemens).

RESULTS

A_{PTV} was quantified by a large volume of interest encompassing all planning target volumes and by setting the PET isocontour threshold to 2% by visual assessment to obtain 1.234 GBq, after decay correction (Fig. 2B). A few small foci of noise artifacts were deemed negligible. $A_{Residual}$ in the delivery apparatus was similarly quantified by setting the PET isocontour threshold to 1% (Fig.2C) to obtain 0.015 GBq, after decay correction (*5*). $A_{Nontarget}$ was undetectable, taken to be zero. A_{Total} was 1.266 GBq measured by a dose calibrator during radiomicrosphere v-vial preparation, after decay correction.

A_{Lung} was therefore $1.266 - (1.234 + 0.015) = 0.017$GBq. Therefore, the true lung shunt fraction was $(0.017/1.266) \times 100$ = approximately 1%. This result was consistent with qualitative bremsstrahlung lung findings and was a vast improvement from the original 26%, objectively affirming technical success and complete lung protection by hepatic vein balloon occlusion. The patient's lung mass, measured by CT densitovolumetry, was 0.85 kg (*7*). D_{Lung} was therefore $50 \times (0.017/0.85)$ = approximately 1 Gy. Clinically, the patient did not develop any respiratory symptoms, and a follow-up MRI scan 2 mo later did not show any evidence of pneumonitis on the routinely acquired high resolution gradient-recalled echo (GRE) T1 and half Fourier single-shot turbo spin-echo (HASTE) T2 sequences, clinically validating our lung protection methods and calculations. Hepatic vein balloon occlusion had also improved the tumor mean absorbed dose from an initial 88 Gy simulated by ^{99m}Tc-MAA predictive dosimetry to a final 101 Gy verified by ^{90}Y PET/CT (Fig. 2D) (*6*). Four-month follow-up MRI showed a mild size reduction of the tumor mass, clinically consistent with the ^{90}Y PET/CT absorbed dose verification.

DISCUSSION

This technical report demonstrates 2 concepts: first, the true lung absorbed dose may be indirectly quantified by ^{90}Y PET/CT, and second, complete lung protection by hepatic vein balloon

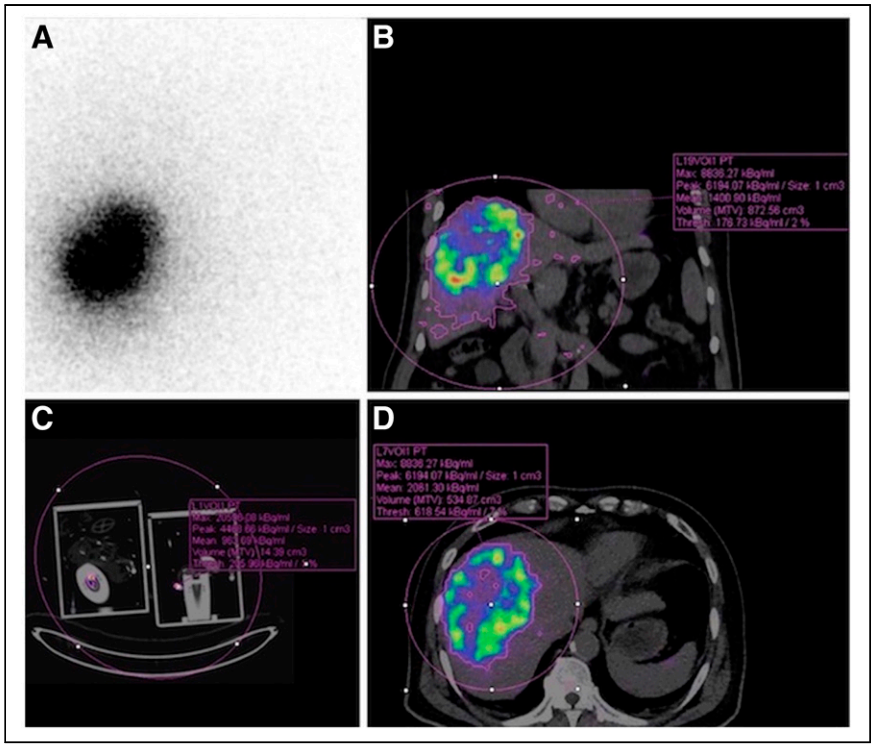

FIGURE 2. (A) Bremsstrahlung planar scintigraphy does not show any visually significant lung activity, a qualitative indication of successful lung protection. (B) ^{90}Y PET/CT with PET isocontour threshold 2% to encompass all activity within planning target volumes. Lungs were outside the PET field of view. Left liver lobe was spared from radioembolization. (C) ^{90}Y PET/CT of delivery apparatus with PET isocontour threshold 1% to encompass all residual activity. (D) ^{90}Y PET/CT with PET isocontour threshold 7% to quantify tumor activity.

occlusion is possible. A recent comprehensive review by Kappadath et al. highlighted the historical pitfalls and limitations in our current methods of lung radiation planning for radioembolization (*1*). These problems with lung dosimetry are attributable to a lack of standardized methods for calculating the lung shunt fraction and lung dosimetry and our incomplete radiobiologic understanding of the true lung tolerance to radiomicrospheres (*1*). Furthermore, our current understanding of an approximately 20- to 25-Gy lung tolerance for ^{90}Y resin microspheres is not wholly applicable to ^{90}Y glass microspheres due to differences in specific activity and tissue biodistribution. As we gradually gain clarity on the true limits of lung tolerance, we will further improve lung predictive dosimetry using normal tissue complication probability (*4*).

In clinical practice, accurate lung dosimetry is important for both preradioembolization predictive dosimetry and also postradioembolization absorbed dose verification. During preradioembolization predictive dosimetry, a common strategy to overcome tumor absorbed dose heterogeneity is to deliberately escalate the prescribed activity up to the limits of normal tissue safety tolerance (*9*). The lung is often the activity-limiting critical organ, and therefore clear knowledge of the true lung tolerance limit is vital to avoid significant radiomicrosphere pneumonitis (*4*). Our method of indirect lung absorbed dose verification could enable us to describe the true lung shunt fraction of different tumor types and establish the true limits of lung tolerance for radiobiologically distinct radiomicrosphere devices.

After radioembolization, lung absorbed dose verification may be clinically important depending on the treatment strategy. Our case of lung protection by hepatic vein balloon occlusion proved to be technically successful; therefore, no further action was required. However, if the lung absorbed dose was unexpectedly found to be dangerously high, immediate action can be initiated to mitigate the risk of developing severe pneumonitis in the ensuing weeks. Such mitigative measures may include corticosteroids, advice on respiratory symptoms, and close outpatient respiratory surveillance in the weeks after radioembolization.

Hepatic vein balloon occlusion is an established technique that may be deployed in situations of high lung shunting (*8*). However, objective proof of technically successful hepatic vein balloon occlusion expressed in terms of a measured absolute reduction in lung activity, lung shunt fraction, or lung absorbed dose has not been described. This report shows that complete lung protection is possible by hepatic vein balloon occlusion, meaning that nearly all injected radiomicrospheres can be retained within the liver to maximize the tumor absorbed dose and avoid unnecessary lung irradiation. This is especially important for hepatocellular carcinoma where the

KEY POINTS

QUESTION: How do we verify the true lung absorbed dose after radioembolization?

PERTINENT FINDINGS: We devised a simple method to indirectly calculate the true lung absorbed dose using postradioembolization ^{90}Y PET/CT. By this method, we showed that hepatic vein balloon occlusion could achieve complete lung protection from hepatopulmonary shunting of radiomicrospheres.

IMPLICATIONS FOR PATIENT CARE: Postradioembolization indirect lung absorbed dose verification is feasible and may benefit patients in terms of mitigating lung radiotoxicity, safety of repeated radioembolization, and research to better define the true limits of lung radiomicrosphere tolerance. By proving that complete lung protection was possible using hepatic vein balloon occlusion, we suggest a possible new paradigm of massive activity radioembolization to benefit radiomicrosphere lobectomy and segmentectomy.

lung shunt fraction is typically higher than liver metastases, which may preclude safe or effective radioembolization. Complete lung protection renders the lung shunt fraction less relevant, allowing massive activities to be infused for radiomicrosphere lobectomy or segmentectomy. With complete lung protection, repeated radioembolization would also be safer because the cumulative lung absorbed dose would be low.

The main dosimetric limitation of our method of indirect quantification is that it can obtain only the true lung mean absorbed dose, to be superseded in the future by lung dose–volume histograms (*4,9*). However, the true lung dose–volume histogram will remain elusive until ^{90}Y PET/CT further improves in acquisition speed, field of view (e.g., total-body PET scanners), and quantitative accuracy to permit direct lung imaging in the routine clinical setting. There were also several technical assumptions in this work. First, we assumed ^{90}Y PET to be quantitatively accurate. Second, we assumed that our visual method of PET isocontour thresholding was reliable to encompass all true ^{90}Y activity, and that all excluded activity was negligible. Third, we assumed that background noise artifacts had negligible effect on clinical dosimetry. However, we felt that these assumptions were reasonable given our prior validation work and years of experience with ^{90}Y PET (*2,3,5*).

CONCLUSION

Indirect lung absorbed dose verification by ^{90}Y PET/CT is feasible and could improve clinical management and our knowledge of lung safety thresholds. Complete lung protection by hepatic vein balloon occlusion is possible, suggesting a new paradigm where the lung shunt fraction is less relevant and permits massive activity radioembolization for radiomicrosphere lobectomy or segmentectomy. Further research is needed to explore these new concepts.

DISCLOSURE

No potential conflict of interest relevant to this article was reported.

REFERENCES

1. Kappadath SC, Lopez BP, Salem R, Lam MGEH. Reassessment of the lung dose limits for radioembolization. *Nucl Med Commun.* 2021;42:1064–1075.
2. Kao YH, Steinberg JD, Tay YS, et al. Post-radioembolization yttrium-90 PET/CT: part 2—dose-response and tumor predictive dosimetry for resin microspheres. *EJNMMI Res.* 2013;3:57.
3. Kao YH, Tan AEH, Lo RHG, et al. Non-target activity detection by post-radioembolization yttrium-90 PET/CT: image assessment technique and case examples. *Front Oncol.* 2014;4:11.
4. Kao YH. Dose-response for yttrium-90 resin microsphere radioembolisation. *Nucl Med Commun.* 2021;42:345–347.
5. Kao YH, Corlett A, Jorna K, Rhodes A, Sivaratnam D. ^{90}Y PET for qualitative and quantitative assessment of residual activity in delivery apparatus after radioembolization. *J Nucl Med Technol.* 2021;49:178–179.
6. Kao YH, Tan AEH, Burgmans MC, et al. Image-guided personalized predictive dosimetry by artery-specific SPECT/CT partition modeling for safe and effective ^{90}Y radioembolization. *J Nucl Med.* 2012;53:559–566.
7. Kao YH, Magsombol BM, Toh Y, et al. Personalized predictive lung dosimetry by technetium-99m macroaggregated albumin SPECT/CT for yttrium-90 radioembolization. *EJNMMI Res.* 2014;4:33.
8. Schiro BJ, Amour ES, Harnain C, Gandhi RT. Management of high hepatopulmonary shunts in the setting of Y90 radioembolization. *Tech Vasc Interv Radiol.* 2019; 22:58–62.
9. Kao YH. Yes, the Holy Gray exists. Learn from modern radioembolisation. *Eur J Nucl Med Mol Imaging.* 2021;48:4115–4117.